Resonance Trimming in Dielectric Resonant Metasurfaces

Jonathan Bar-David, Noa Mazurski, and Uriel Levy

(Invited Paper)

***Abstract*—The field of metasurfaces is rapidly growing. Nowadays, metasurfaces are considered at the front of artificial optical materials. With metasurfaces, it is possible to control the properties of light for variety of applications, from beam shaping, structural colors, and polarization control to tight focusing, scanning, spatial and spectral filtering, etc. One of the major challenges in the construction of metasurfaces is the need for precise control over their dimensions and consequently their spectral response. In this paper, we demonstrate an approach for postfabrication trimming of dielectric metasurfaces consisting of amorphous silicon layer on top of a quartz substrate, by using local oxidation of silicon technique. The oxidation effectively reduces the radius of the silicon disk, resulting in a blue shift in the observed spectral response. Blue shift of up to 100 nm is demonstrated. Relaxing fabrication tolerances and enabling post-processing techniques is expected to play an important role in promoting the scientific advances of metasurfaces into viable and useful technology. We thus believe that the demonstrated approach will provide an additional important tool to the rapidly developed toolkit of metasurface science and technology.**

***Index Terms*—Dielectric metasurface, Huygens metasurface, LOCOS, post-process.**

I. Introduction

METASURFACES are the subject of flourishing research with variety of configurations and material systems that are being explored [1]–[12]. In recent years, resonant, all-dielectric nanoantennas are researched extensively and the richness of optical phenomena is explored and utilized [1]–[5], [7], [8], [13]–[19]. The superior transmission, low loss, and multiple resonances of such antennas (when compared to metallic counterparts) makes them promising candidates for future optical devices such as holograms and lenses [9], [20]–[23], and color printing [3], [6], [24]–[26]. In this context, semiconductor nanoantennas are of special interest, primarily due to their high refractive index, as well as their physical and chemical stability [7], [8], [13], [14], [27]–[30]. Although semiconductor fabrication techniques are well established, the realization of semiconductor nanoantennas with accurate and desired spectral response is still challenging due to their small dimensions and the need for strict fabrication tolerances dictated by the nanoantennas' resonant nature.

As shown by Mie [8], [31], [32], dielectric optical nanoantennas support two sets of electromagnetic resonances, being the electric and magnetic multipole resonances. For excitation with photon-energies lower than the material band-gap, each of these resonances is typically characterized by high reflection, low transmission, and negligible absorption. The performance metrics such as resonance frequency and coupling can be controlled by the antenna's size and shape, as well as by the antenna's refractive index and the index contrast between the antenna and surrounding medium [7], [13], [16], [17], [33]. These properties are set during the fabrication process and can barely be changed post fabrication, unless some active approaches are being used [14], [15], [22], [34], [35].

In this letter we propose and experimentally demonstrate a fabrication method exploiting the natural chemical properties of semiconductor material, which allows post fabrication trimming of the spectral characteristics of silicon nanoantennas. The approach allows to relax the tight fabrication tolerances of dielectric metasurfaces and provide a "knob" for tailoring their response based on the design and the desired application. By doing so, one can either tailor a mis-fabricated device towards the desired spectral band, or alternatively, modify the device functionality towards a different spectral band without the need of fabricating a new device.

II. Fabrication

Fabrication of dielectric metasurfaces which allow trimming is sketched in Figure 1. Our method is based on the LOCOS technique reported previously [30], [36]–[40]. We begin by depositing the nanoantenna layer consisting of a 275 nm thick a-Si layer (PECVD, Oxford) on top of a quartz substrate. Atop the a-Si layer we deposit a 150 nm thick Si_3N_4 (silicon nitride) layer, which will later act as an oxidation mask. The nanoantennae patterns are then defined by spin-coating of an electron beam resist (ZEP 520A) followed by electron beam lithography (Raith

Manuscript received August 16, 2018; revised December 22, 2018; accepted February 20, 2019. Date of publication March 4, 2019; date of current version March 28, 2019. This work was supported by the Israeli Ministry of Science and Technology. The work of J. Bar-David was supported by the Applied Science and Engineering Fellowship from the Israeli Ministry of Science and Technology. *(Corresponding author: Uriel Levy.)*

The authors are with the Department of Applied Physics, Benin School of Engineering and Computer Science, Center for Nanoscience and Nanotechnology, The Hebrew University of Jerusalem, Jerusalem 91904, Israel (e-mail: jonathan.bardavid@mail.huji.ac.il; noam@savion.huji.ac.il; ulevy@mail.huji.ac.il).

This paper has supplementary downloadable material available at http://ieeexplore.ieee.org, provided by the authors.

Color versions of one or more of the figures in this paper are available online at http://ieeexplore.ieee.org.

Digital Object Identifier 10.1109/JSTQE.2019.2902911

1077-260X © 2019 IEEE. Personal use is permitted, but republication/redistribution requires IEEE permission.
See http://www.ieee.org/publications_standards/publications/rights/index.html for more information.

Authorized licensed use limited to: Hebrew University. Downloaded on July 29,2020 at 20:25:31 UTC from IEEE Xplore. Restrictions apply.

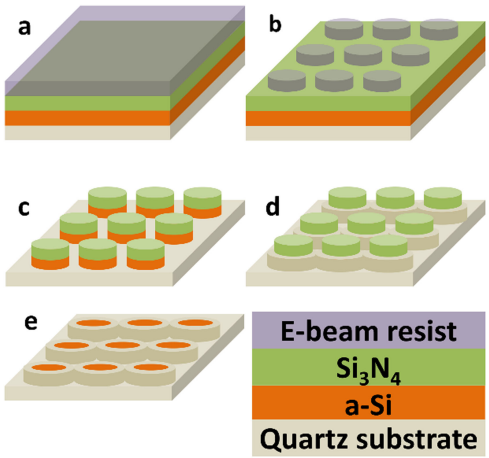

Fig. 1. Metasurface fabrication process. (a) a-Si and Si_3N_4 are deposited on a quartz substrate and Ebeam resist is spin-coated on top (b) Sample patterning by Ebeam lithography. (c) The sample is etched, allowing for pattern transfer into the dielectric layers. (d) Sample oxidization. The Si_3N_4 layer acts as oxidation mask to prevent nanoantennas from completely oxidizing. (e) Si_3N_4 layer is removed to obtain the final structure.

Eline). The pattern is transferred to the Si_3N_4 and a-Si silicon by reactive ion etch (Corial) with a mixture of SF_6 (etchant) with CHF_3 and O_2 (inhibitors). After etching, the remaining ZEP is stripped, and the sample is oxidized in a furnace in wet environment, resulting in an oxide ring of about 50–100 nm in width, as depicted in figure 1(d) and 2(b). The precise trimming of the resonance is accomplished by controlling the oxidation time and temperature. The results reported here were obtained by oxidizing the sample for approx. 30 minutes in a temperature of ∼900 °C in a H_2O atmosphere, which produces a 100 nm thick oxide layer on a flat crystalline silicon substrate serving as a reference. SEM micrograph of the fabricated metasurface (cylindrical nanoantennas in hexagonal lattice) is presented in Figure 2(a) shows the metasurface etching but before oxidation, demonstrating the process towards obtaining the final structure. Finally, Figure 2(b) shows the final metasurface after oxidation and Si_3N_4 removal. A close examination of Figure 2(a) shows thin connection "bridges" between adjacent nanoantennas. This is a result of the shortcoming of the RIE process to properly etch trenches of small width. As seen in Figure 2(b), these "bridges" are likely to be fully oxidized, therefore their effect on the optical properties is expected to be negligible.

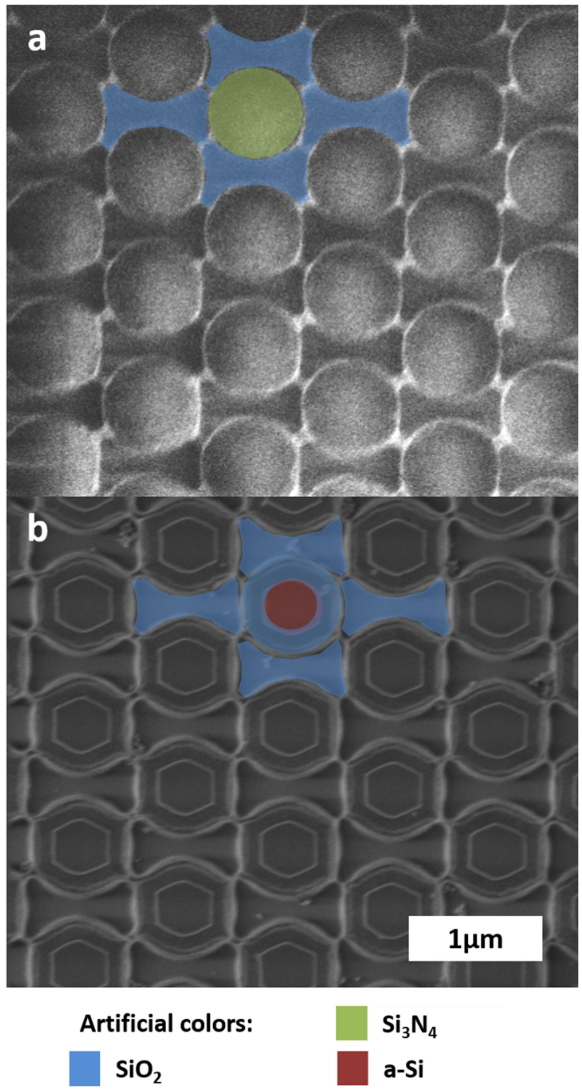

Fig. 2. Metasurface SEM micrograph. (a) Nanoantenna array after etching. Residual silicon "bridges" were not etched and are seen as connections between adjacent nanoantennas. (b) The same nanoantenna array as in (a), after oxidation and Si_3N_4 removal. The disk size (red) is significantly smaller as compared to the original size (green). Moreover, silicon bridges seem to be fully oxidized. Scale bar is the same for both images.

III. Characterization

We have fabricated few sets of samples consisting of cylinders of amorphous silicon (a-Si) on top of quartz substrate. Each of the fabricated samples were measured three times during the fabrication process: 1 - after etching through Si_3N_4 and a-Si layers, 2 - after oxidation, and 3 - after removing the Si_3N_4 layer (i.e., when the fabrication process is completed). By doing so, we can isolate the effect of each process step on the transmitted spectrum.

The optical properties were characterized by transmission spectroscopy (as reported in ref [30]): white light emerging from a Tungsten Halogen source illuminates the sample and is collected through a 50X microscope objective (Nikon) and then coupled to a multimode fiber leading to the input of a spectrometer (Horiba, microHR). The obtained spectra are compared to 3D FDTD simulations of the fabricated structures (Lumerical FDTD solver, Lumerical Inc.)

Results of our optical characterization are presented in Figures 3 and 4. While typically both the dipole and the quadrupole modes are excited, we have chosen to focus on the quadrupole mode which is conveniently located within the wavelength band that is characterized, as can be clearly observed in Figures 3 and 4. The quadrupole mode is denoted by the dashed line (Figure 3(a–e)) which indicates the spectral shift it undergoes as a function of the nano antenna radius and within the various fabrication steps. Figure 3 presents the measured (left panel) and simulated

Authorized licensed use limited to: Hebrew University. Downloaded on July 29,2020 at 20:25:31 UTC from IEEE Xplore. Restrictions apply.

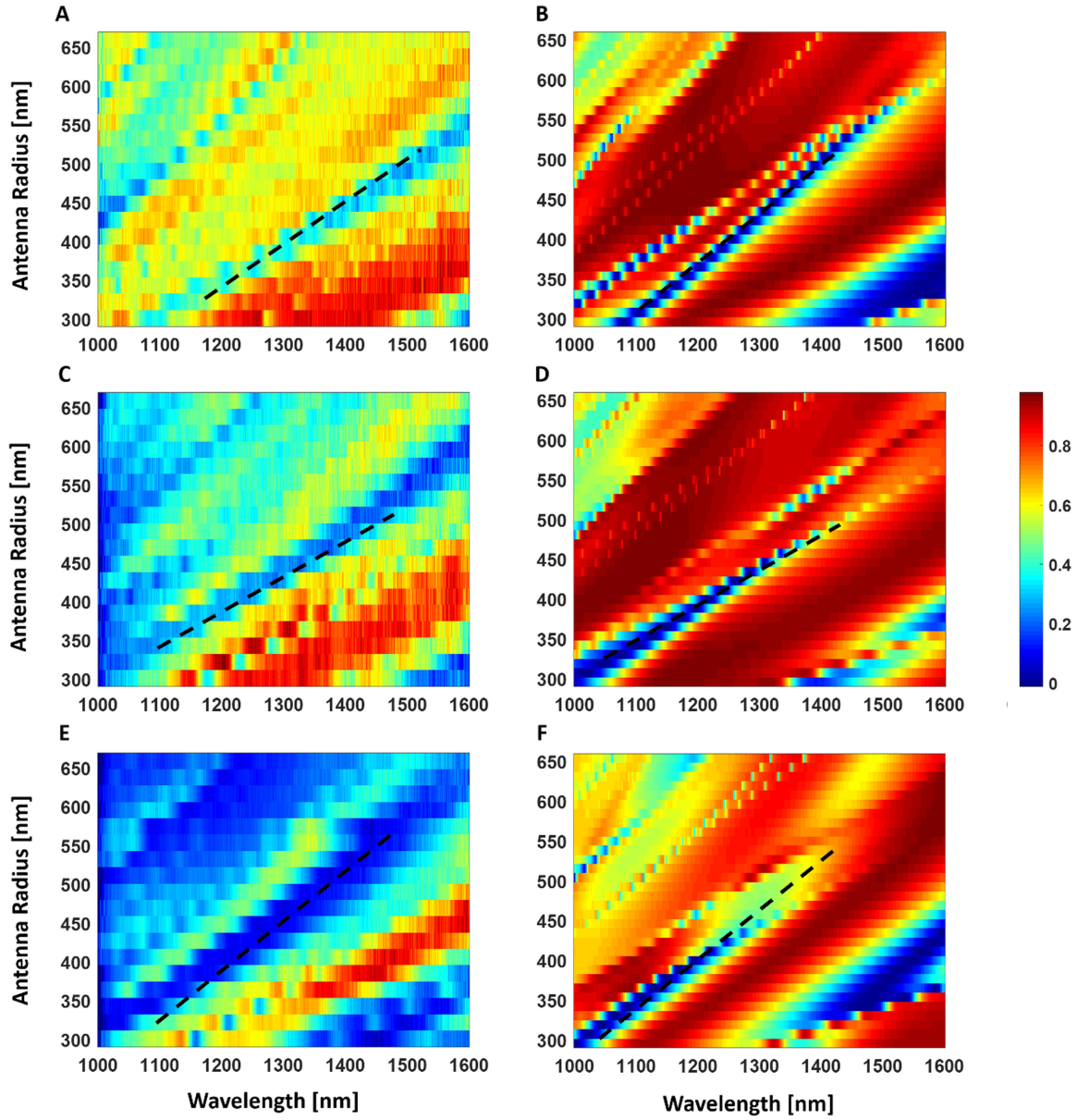

Fig. 3. Transmission spectra for nanoantenna arrays (color bar for all maps on the right). The dashed lines follow the pronounced electric quadrupole mode of the nanoantennas, which redshifts as nanoantenna radii grow along the y-axis and blue-shifts as a result of oxidation and nitride removal. (a-b) Measured and simulated (respectively) spectra for the nanoantenna arrays after the etch step, and before oxidation. (c-d) Measured and simulated spectra for metasurfaces after the etch step and oxidation. The quadrupole mode is blue-shifted significantly due to the shrinking of the silicon antenna radius. (e-f) Same as (c-d) with the additional step of Si_3N_4 layer removal. The quadrupole mode is further blue-shifted. The array is implemented as a hexagonal grid with constant gap of 200 nm between adjacent cylinders.

(right panel) transmission spectra for different process stages. The top row (Fig. 3a, b) corresponds to the measured and the simulated transmission spectra of the sample after etching, prior to oxidation. The middle row (Fig. 3c, d) corresponds to the measured and the simulated transmission spectra of the sample after etching and oxidation, whereas the lower row (Fig. 3e, f) corresponds to the measured and the simulated transmission spectra of the sample after etching, oxidation, and nitride removal. In general, one can observe the similarity between the measured and the simulated spectra for all three cases. Slight discrepancies are attributed to the detailed shape of the nanoantennas which could not be fully accounted for in the simulations and to variations in oxide thickness due to change in oxidation rates for different structures. Nevertheless, the expected blue-shift of resonant frequencies between the three fabrication steps can be clearly observed in both measured and simulated spectra.

To emphasis this blue-shift, we have plotted (Fig. 4) two selected cross sections of Fig. 1, corresponding to the transmission spectrum of an array with radii of 300 nm (Fig. 4 top row) and 450 nm (Fig. 4, lower row). As inferred from Figure 4, the major

Authorized licensed use limited to: Hebrew University. Downloaded on July 29,2020 at 20:25:31 UTC from IEEE Xplore. Restrictions apply.

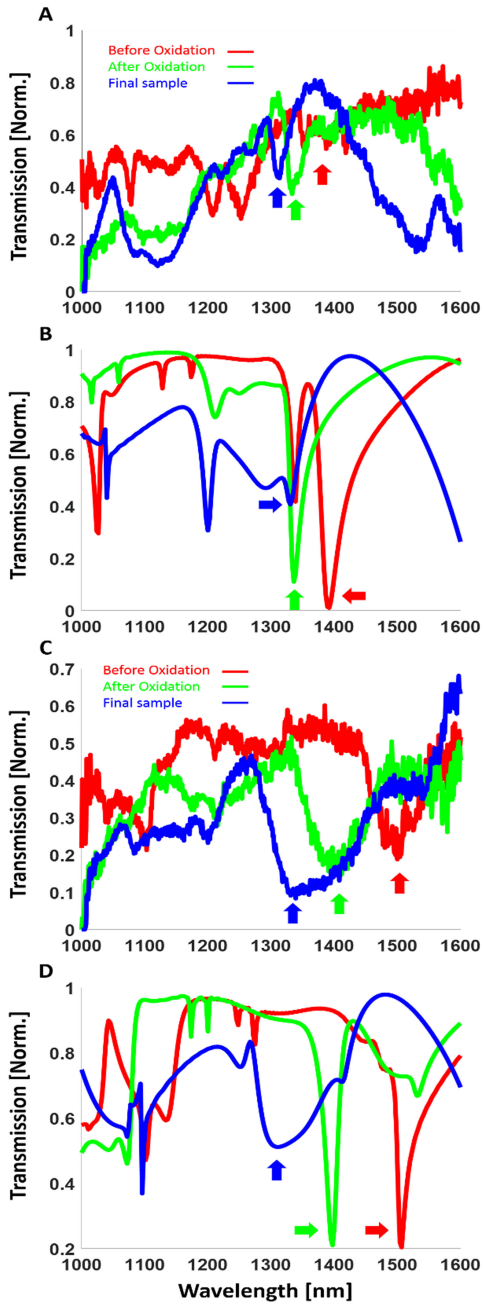

Fig. 4. Plots of specific cross sections of Figure 3. (a-b) Measured and simulated spectra for nanoantenna array with radius of ∼360 nm. Colored arrows are added as guides to the eye to denote the electric quadrupole resonance in all measurements and simulations. (c-d) Measured and simulated spectra for nanoantennas of radius 450 nm. Red – structure after etching and before oxidation. Green – structure after etching and oxidation. Blue, the final structure after nitride removal.

blue-shift occurs between the non-oxidized stage and the oxidized stage: the oxide layer is fairly large as compared to overall diameter and its refractive index is drastically different from the refractive index of a-silicon. Therefore, the resonant wavelength is blue-shifted by ∼100 nm. This is a major shift in resonance frequency which corresponds to about 60 nm difference in the etched disk radius, much larger than needed to accommodate for fabrication errors. The remaining blue shift occurring by removing the Si_3N_4 oxidation mask is weaker, as the main effect is the increase in index contrast between the antenna and the surrounding air rather than a real change in geometry.

IV. Discussion and Outlook

We have demonstrated the post fabrication trimming of dielectric metasurfaces consisting of amorphous silicon layer on top of a quartz substrate. Trimming is achieved by the use of local oxidation of silicon (LOCOS) technique [30], [36]–[40], which effectively reduces the radius of the silicon disk, resulting in a blue shift in the observed spectral response. Blue shift of about 100 nm has been achieved via oxidation of about 30 minutes at a temperature of ∼900 °C. As current-day metasurface fabrication relies on advanced fabrication techniques with low tolerances and limited throughput [20], [23], relaxing fabrication tolerances and enabling advanced post-processing is expected to play an important role in promoting the scientific advances of metasurfaces into viable and useful technology. In the case of metasurfaces, this has special importance as the resonant phenomena is primarily affected by the radius of the cylinder. We thus believe that the demonstrated approach will provide another tool to the rapidly developed toolkit of metasurface science and technology.

Appendix

A supplementary information file is published with this report. The supplementary contains refractive index measurements of Si before and after oxidation processes as well as simulation results of the electric fields of the resonant modes discusses above.

References

[1] L. Novotny and N. van Hulst, "Antennas for light," *Nature Photon.*, vol. 5, no. 2, pp. 83–90, Feb. 2011.
[2] A. I. Kuznetsov, A. E. Miroshnichenko, M. L. Brongersma, Y. S. Kivshar, and B. Luk'yanchuk, "Optically resonant dielectric nanostructures," *Science*, vol. 354, no. 6314, Nov. 2016, Art. no. 2472.
[3] A. Kristensen *et al.*, "Plasmonic colour generation," *Nature Rev. Mater.*, vol. 2, Nov. 2016, Art. no. 16088.
[4] N. Yu and F. Capasso, "Flat optics with designer metasurfaces," *Nature Mater.*, vol. 13, no. 2, pp. 139–150, Feb. 2014.
[5] A. B. Evlyukhin *et al.*, "Demonstration of magnetic dipole resonances of dielectric nanospheres in the visible region," *Nano Lett.*, vol. 12, no. 7, pp. 3749–3755, Jul. 2012.
[6] J. S. Clausen *et al.*, "Plasmonic metasurfaces for coloration of plastic consumer products," *Nano Lett.*, vol. 14, no. 8, pp. 4499–4504, Aug. 2014.
[7] I. Staude *et al.*, "Tailoring directional scattering through magnetic and electric resonances in subwavelength silicon nanodisks," *ACS Nano*, vol. 7, no. 9, pp. 7824–7832, Sep. 2013.
[8] P. P. Iyer, N. A. Butakov, and J. A. Schuller, "Reconfigurable semiconductor phased-array metasurfaces," *ACS Photon.*, vol. 2, no. 8, pp. 1077–1084, Jun. 2015.
[9] Z. Bomzon, G. Biener, V. Kleiner, and E. Hasman, "Space-variant Pancharatnam–Berry phase optical elements with computer-generated subwavelength gratings," *Opt. Lett.*, vol. 27, no. 13, pp. 1141–1143, Jul. 2002.
[10] Z. Bomzon, V. Kleiner, and E. Hasman, "Pancharatnam–Berry phase in space-variant polarization-state manipulations with subwavelength gratings," *Opt. Lett.*, vol. 26, no. 18, pp. 1424–1426, Sep. 2001.
[11] G. Li *et al.*, "Metasurface holograms reaching 80% efficiency," *Nature Nanotechnol.*, vol. 10, no. 4, pp. 308–312, Apr. 2015.
[12] S. Keren-Zur, O. Avayu, L. Michaeli, and T. Ellenbogen, "Nonlinear beam shaping with plasmonic metasurfaces," *ACS Photon.*, vol. 3, no. 1, pp. 117–123, Jan. 2016.
[13] M. Decker *et al.*, "High-efficiency dielectric Huygens' surfaces," *Adv. Opt. Mater.*, vol. 3, no. 6, pp. 813–820, Jun. 2015.

Authorized licensed use limited to: Hebrew University. Downloaded on July 29,2020 at 20:25:31 UTC from IEEE Xplore. Restrictions apply.

[14] T. Lewi, P. P. Iyer, N. A. Butakov, A. A. Mikhailovsky, and J. A. Schuller, "Widely tunable infrared antennas using free carrier refraction," *Nano Lett.*, vol. 15, no. 12, pp. 8188–8193, Dec. 2015.
[15] I. Brener, X. Miao, E. A. Shaner, B. S. Passmore, and Y. C. Jun, "Mid-infrared tunable metamaterials," U.S. Patent 9018 642 B1, Apr. 28, 2015.
[16] N. A. Butakov and J. A. Schuller, "Designing multipolar resonances in dielectric metamaterials," *Sci. Rep.*, vol. 6, Dec. 2016, Art. no. 38487.
[17] A. I. Kuznetsov, A. E. Miroshnichenko, Y. H. Fu, J. Zhang, and B. Luk'yanchuk, "Magnetic light," *Sci. Rep.*, vol. 2, Jul. 2012, Art. no. 492.
[18] P. Moitra *et al.*, "Realization of an all-dielectric zero-index optical metamaterial," *Nature Photon.*, vol. 7, no. 10, pp. 791–795, Oct. 2013.
[19] P. Moitra *et al.*, "Large-scale all-dielectric metamaterial perfect reflectors," *ACS Photon.*, vol. 2, no. 6, pp. 692–698, Jun. 2015.
[20] W. T. Chen *et al.*, "Immersion meta-lenses at visible wavelengths for nanoscale imaging," *Nano Lett.*, vol. 17, no. 5, pp. 3188–3194, May 2017.
[21] B. Desiatov, N. Mazurski, Y. Fainman, and U. Levy, "Polarization selective beam shaping using nanoscale dielectric metasurfaces," *Opt. Express*, vol. 23, no. 17, pp. 22611–22618, Aug. 2015.
[22] J. Bar-David, L. Stern, and U. Levy, "Dynamic control over the optical transmission of nanoscale dielectric metasurface by alkali vapors," *Nano Lett.*, vol. 17, no. 2, pp. 1127–1131, Feb. 2017.
[23] R. Paniagua-Dominguez *et al.*, "A metalens with near-unity numerical aperture," *Nano Lett.*, vol. 18, pp. 2124–2132, Mar. 2018.
[24] X. Zhu, W. Yan, U. Levy, N. A. Mortensen, and A. Kristensen, "Resonant laser printing of structural colors on high-index dielectric metasurfaces," *Sci. Adv.*, vol. 3, no. 5, May 2017, Art. no. e1602487.
[25] K. Kumar *et al.*, "Printing colour at the optical diffraction limit," *Nature Nanotechnol.*, vol. 7, no. 9, pp. 557–561, Sep. 2012.
[26] Y. Nagasaki, M. Suzuki, I. Hotta, and J. Takahara, "Control of Si-based all-dielectric printing color through oxidation," *ACS Photon.*, vol. 5, no. 4, pp 1460–1466, Jan. 2018.
[27] S. Law, L. Yu, A. Rosenberg, and D. Wasserman, "All-semiconductor plasmonic nanoantennas for infrared sensing," *Nano Lett.*, vol. 13, no. 9, pp. 4569–4574, Sep. 2013.
[28] J. H. Lee *et al.*, "A semiconductor metasurface with multiple functionalities: A polarizing beam splitter with simultaneous focusing ability," *Appl. Phys. Lett.*, vol. 104, no. 23, Jun. 2014, Art. no. 233505.
[29] S. Liu, G. A. Keeler, J. L. Reno, M. B. Sinclair, and I. Brener, "III-V semiconductor nano-resonators-a new strategy for passive, active, and nonlinear all-dielectric metamaterials," *Adv. Opt. Mater.*, vol. 4, pp. 1658–1658, 2016.
[30] J. Bar-David, N. Mazurski, and U. Levy, "In situ planarization of Huygens metasurfaces by nanoscale local oxidation of silicon," *ACS Photon.*, vol. 4, no. 9, pp. 2359–2366, Sep. 2017.
[31] G. Mie, "Beiträge zur Optik trüber Medien, speziell kolloidaler Metallösungen," *Ann. Phys.*, vol. 330, no. 3, pp. 377–445, Jan. 1908.
[32] C. F. Bohren and D. R. Huffman, *Absorption and Scattering of Light by Small Particles*. Hoboken, NJ, USA: Wiley, 2008.
[33] K. E. Chong *et al.*, "Observation of Fano resonances in all-dielectric nanoparticle oligomers," *Small*, vol. 10, no. 10, pp. 1985–1990, May 2014.
[34] Y.-W. Huang *et al.*, "Gate-tunable conducting oxide metasurfaces," *Nano Lett.*, vol. 16, no. 9, pp. 5319–5325, Sep. 2016.
[35] A. Forouzmand, M. M. Salary, S. Inampudi, and H. Mosallaei, "A tunable multigate indium-tin-oxide-assisted all-dielectric metasurface," *Adv. Opt. Mater.*, vol. 6, no. 7, Apr. 2018, Art. no. 1701275.
[36] A. Naiman *et al.*, "Ultrahigh-Q silicon resonators in a planarized local oxidation of silicon platform," *Opt. Lett.*, vol. 40, no. 9, pp. 1892–1895, May 2015.
[37] I. Goykhman, B. Desiatov, J. Khurgin, J. Shappir, and U. Levy, "Locally oxidized silicon surface-plasmon Schottky detector for telecom regime," *Nano Lett.*, vol. 11, no. 6, pp. 2219–2224, Jun. 2011.
[38] I. Goykhman, B. Desiatov, and U. Levy, "Experimental demonstration of locally oxidized hybrid silicon-plasmonic waveguide," *Appl. Phys. Lett.*, vol. 97, no. 14, Oct. 2010, Art. no. 141106.
[39] F. Y. Gardes *et al.*, "Sub-micron optical waveguides for silicon photonics formed via the local oxidation of silicon (LOCOS)," *Proc. SPIE*, vol. 6898, 2008, Art. no. 68980R.
[40] M. P. Nezhad, O. Bondarenko, M. Khajavikhan, A. Simic, and Y. Fainman, "Etch-free low loss silicon waveguides using hydrogen silsesquioxane oxidation masks," *Opt. Express*, vol. 19, no. 20, pp. 18827–18832, Sep. 2011.

Jonathan Bar-David received the B.Sc. degree in physics and the M.Sc. degree in applied physics from The Hebrew University of Jerusalem, Jerusalem, Israel, where he is currently working toward the Ph.D. degree in applied physics with the NanoOpto Group.

Noa Mazurski received the B.E. degree in chemical engineering and the M.E. degree in environmental engineering from the Technion – The Israeli Institute of Technology, Haifa, Israel.

She is currently a Process Engineer and Nanofabrication Expert with the NanoOpto Research Group, The Hebrew University of Jerusalem, Jerusalem, Israel .

Uriel Levy received the B.E.Sc. degree in physics and material engineering from the Technion – The Israeli Institute of Technology, Haifa, Israel, and the Ph.D. degree in electrical engineering from Tel Aviv University, Tel Aviv, Israel.

He conducted postgraduate research at the University of California, San-Diego, CA, USA. Since 2006, he has been a Professor in applied physics and the Head of the NanoOpto Research Group with The Hebrew University of Jerusalem, Jerusalem, Israel.

Authorized licensed use limited to: Hebrew University. Downloaded on July 29,2020 at 20:25:31 UTC from IEEE Xplore. Restrictions apply.